Nuclear Instruments and Methods in Physics Research B 412 (2017) 34–40

Contents lists available at ScienceDirect

Nuclear Instruments and Methods in Physics Research B

journal homepage: www.elsevier.com/locate/nimb

Cross sections for proton-induced reactions on ^{nat}Sb up to 68 MeV

M.A. Mosby [a], E.R. Birnbaum [a], F.M. Nortier [a], J.W. Engle [a,b,*]

[a] Los Alamos National Laboratory, P.O. Box 1663, Los Alamos, NM 87545, United States
[b] University of Wisconsin School of Medicine and Public Health, 1111 Highland Avenue, Madison, WI 53711, United States

ARTICLE INFO

Article history:
Received 17 August 2017
Received in revised form 29 August 2017
Accepted 30 August 2017

Keywords:
Cross section
^{119}Te
^{119}Sb
^{117m}Sn
^{119}Te/^{119}Sb generator
Proton
Radionuclide production
Radiotherapy
Auger electron

ABSTRACT

Nuclear excitation functions for proton induced reactions on antimony targets have been measured up to 68 MeV using stacked foil activation techniques at the Crocker Laboratory of the University of California at Davis. Measurements made are expected to be useful in production of therapeutic radionuclides ^{119}Sb (via production of its parents ^{119m}Te and ^{119g}Te) and ^{117m}Sn. This work extends the energy coverage of available data upwards by approximately 30 MeV into a range relevant to medium-energy radionuclide production facilities like the Isotope Production Facility in Los Alamos, New Mexico and the Brookhaven Linear Isotope Producer in Upton, New York.

1. Introduction

Proton induced reactions on targets of natural antimony are of interest to the isotope community as there are several nuclides produced in these reactions useful for either therapy or diagnostic purposes. There has been interest in the use of various radionnuclides for therapeutic purposes, as the range of these low-energy electrons in matter is extremely short, allowing for precision targeting of tumor cells with no damage to surrounding tissue (see, e.g., [1,2] and references therein). This makes Auger-emitters ideal for treatment of micro metastases. The radionuclide ^{119}Sb is of particular interest, as the spectrum of electrons it emits is of a more moderate energy, with several conversion electrons whose mean free path in tissue is small enough to stay within an individual cancer cell, but long enough to avoid the need to target the cell nucleus or even directly bind DNA itself [3,4]. The radionuclide ^{117m}Sn is also produced by proton irradiation of antimony targets and is appealing because its Auger-emitting decays are accompanied by emission of a SPECT-imagable 159 keV gamma [5,6].

Cross section measurements have been made up to 50 MeV (see especially [7] and references therein), but there are inconsistencies between the published measurements. Additionally, there is no nuclear data available at higher energies which are of interest to the Isotope Production Facility (IPF) at Los Alamos National Laboratory (LANL), where protons up to 100 MeV are available for radioisotope production. Cross section measurements were made using the cyclotron at the Crocker Nuclear Laboratory (CNL) at the University of California at Davis up to 68 MeV and are reported here.

2. Materials and methods

Measurements were made at the 76-inch cyclotron at the CNL. Proton beam energies of up to 68 MeV are available at this facility. Two irradiations were done in this experiment, one at 68 MeV for one hour and one at 35 MeV for 1.5 h. In each irradiation, a target stack was assembled consisting of Sb foils interspersed with monitor foils and Al degraders. These foils were then assayed by gamma spectrometry to determine total radionuclide yield.

2.1. Irradiation and gamma spectrometry

In the first irradiation, a proton beam of nominal energy 68 MeV at roughly 40 nA was impinged on a target stack, consisting of a series of Kapton-covered foils of Sb, Al, and Cu. Between each set of foils, an Al degrader was used to decrease the beam energy,

* Corresponding author at: B1303 WIMR Cyclotron Laboratory, 1111 Highland Avenue, Madison, WI 53711, United States.
E-mail address: jwengle@wisc.edu (J.W. Engle).

http://dx.doi.org/10.1016/j.nimb.2017.08.038
0168-583X/

and the stack was irradiated for roughly 1 h. After a 3 h cooling period, the foil stack was disassembled, and the individual foils were counted on a high purity germanium (HPGe) detector which was transported from LANL to CNL for this purpose. A similar procedure was repeated for the 35 MeV irradiation. The proton beam was impinged on the target stack of Sb, Ti, and Cu foils at 75 nA for about 1.5 h. The target chamber was allowed to cool for 2 h, and the foils were again counted on the HPGe detector at CNL. The HPGe detectors used to assay the foils are p-type aluminum windowed ORTEC GEM detectors with a relative efficiency at 1333 keV of about 10% and a measured gamma peak FWHM at 1333 keV of 2.05 keV (CNL) and 1.99 keV (LANL), both calibrated daily.

The beamline at the UC Davis cyclotron lacked a real-time, calibrated method of tracking the beam current to provide an integrated proton fluence over the time of irradiation. The monitor foils inserted in the target stack were used to determine the time-averaged flux during the irradiation. These numbers were compared to crude output from a secondary emission electron monitor (SEEM) to validate the approximate magnitude of the fluence during the irradiations. A linear fit to the observed fluence as a function of position of the monitor foil in the foil stack was used to determine the fluence from each ^{nat}Sb foil. The reactions used for the quantification of the fluence are tabulated in Table 1. The initial energy of the proton beam was determined from settings of the cyclotron steering magnets. Incident energies at each foil were calculated using Anderson & Ziegler's semi-empirical energy loss formalism [8].

After several days of counting, the foils were shipped to the LANL Nuclear and Radiochemistry (C-NR) counting room for further gamma spectrometry analysis on an HPGe system with automated sample changer. The net photopeak areas from both the counts at CNL and LANL were analyzed as a function of time to determine the decay curve for each observed radionuclide. The decay curve was then used to extrapolate the activity of each radionuclide present at the end of the two irradiations, A0.

2.2. Nuclear data

The nuclear data used in this analysis is tabulated in Table 2. The same procedure was used to determine product yields for the monitor foil reactions. The cross sections used in this case are those recommended by the IAEA for established monitor reactions ^{27}Al(p,x)^{22}Na, ^{nat}Cu(p,x)^{62}Zn, ^{nat}Cu(p,x)^{56}Co, and ^{nat}Ti(p,x)^{48}V [9], used here to verify the beam energy and determine the proton beam current at each foil location, thereby allowing for a calculation of the production cross section for each radioisotope at discrete energies.

The ^{nat}Sb foils were analyzed in the same way as the monitor foils, with gamma spectrometry being used to determine the photopeak area for each decay as a function of time from end of irradiation. For most observed nuclei, there were no overlapping decays or feeding from higher-lying states. The total number of nuclei present at the end of irradiation was calculated by logarithmic fit to the measured decay curve with extrapolation to the end of irradiation.

Table 1
Reactions used as monitor foils for each irradiation.

Monitor Reaction	E_0 = 68 MeV	E_0 = 35 MeV
^{27}Al(p,x)^{22}Na	x	
^{nat}Cu(p,x)^{56}Co	x	
^{nat}Cu(p,x)^{62}Zn	x	x
^{nat}Ti(p,x)^{48}V		x

2.3. Error analysis

Uncertainties in the fitted logarithmic parameters were computed as the standard error in the activity extrapolated to the end of bombardment. This value was combined according to the Gaussian law of error propagation with estimated contributing uncertainties from detector calibration and geometry reproducibility (4.8% combined), target foil dimensions (0.1%), and proton flux (7.9%). Additional uncertainty was incorporated as the fitted full width at half maximum of the Gaussian-broadened energy distribution at each successive foil in the stack. These uncertainties were combined according to the Gaussian law of error propagation to arrive at an estimate of the total uncertainty of a given value.

3. Results and discussion

All measured data are summarized below in Tables 3 and 4. Individual discussions of measured data follow, but some general comments can be made concerning agreement with previously published data. First, the recent measurements of Takacs et al. [7] are frequently in good or excellent agreement with data reported here. This is in contrast to the most comprehensive datasets published prior to 2015, which seem to exhibit frequent displacement from our values both in energy and in the magnitude of the cross section [11,12], often in a manner that makes the disagreement impossible to explain satisfactorily with methodological scrutiny. In a few instances, additional data do exist [13–16], but only Elbinawi et al. [16] offers useful corroboration of other measured data. The reader is referred to useful discussions of cross section types, "cumulative" and "independent", used below, from prior publications: [17,18].

3.1. ^{123m}Te, ^{117m}Sn, and ^{117}Sb

Each of these three radionuclides have principle gamma emissions near 159 keV. The half-life of ^{117}Sb is 2.8 h, in comparison to 119.2 d for ^{123m}Te and 14.0 d for ^{117m}Sn. To avoid contaminating the measured signal for ^{123m}Te and ^{117m}Sn with emissions from ^{117}Sb, only counts from after the shipment to LANL were considered, meaning the foils had cooled for two (35 MeV stack) or three (68 MeV stack) days. As the remaining nuclei have quite disparate half-lives, the decay curve was fit with a 2-parameter logarithmic decay equation to give the initial quantities of ^{123m}Te and ^{117m}Sn at the end of irradiation. To determine the quantity of ^{117m}Sn present at end of irradiation, a 3-parameter logarithmic decay fit was done, with 2 parameters fixed at the initial quantities of ^{123m}Te and ^{117m}Sn. Quantification of the ^{117}Sb was performed using the initial activities of ^{123m}Te and ^{117}Sn as fixed parameters in a one-component fit of photopeak data collected between the end of irradiation and shipment of the foils to Los Alamos. This work represents, to our knowledge, the first "thin-target" measurement of proton-induced excitation functions for the exciting therapeutic radionuclide ^{117m}Sn, and suggests that it can be co-produced along with radioisotopes of antimony, by proton irradiations with a few tens of MeV incident energy.

Measured excitation functions for ^{123m}Te are presented in Fig. 1, for ^{117m}Sn in Fig. 2, and for ^{117}Sb in Fig. 3 below. The theoretical predictions of the TALYS code documented in the TENDL-2015 library [19] and the measured data of Elbinawi [16] are consistent with values reported here and the data from Takacs et al. [7] below 20 MeV. Above 20 MeV, the Takacs data are higher than those reported here. Other datasets are notably discrepant from each other and with our measured values.

Table 2
Nuclear data used for radioisotopes of antimony, tellurium and tin in this work.s.

Nucleus	Half Life	Decay Mode	E_γ (keV)	γ abundance (%)
^{123m}Te	119.2 d	100% IT	159.0	84.0
^{121m}Te	164.2 d	11.4% EC	1002.1	2.5
		88.6 IT	212.2	81.5
^{121g}Te	19.2 d	100% EC	470.5	1.4
			573.1	80.4
^{119m}Te	4.7 d	100% EC	153.6	66.0
			270.5	28.0
			1212.7	66.1
^{119g}Te	16.1 h	100% EC	644.0	84.1
			699.9	10.1
^{118}Te	6.0 d	100% EC	no gamma	
^{122g}Sb	2.7 d	97.59% β^-	564.2	70.7
		2.4% EC	692.7	3.0
^{120m}Sb	5.8 d	100% EC	197.3	87.0
			1023.3	99.4
			1171.3	100.0
^{118m}Sb	5.0 h	100% EC	253.7	99.0
			1050.7	97.0
			1229.7	100.0
^{117}Sb	2.8 h	100% EC	158.6	85.9
^{117m}Sn	14.0 d	100% IT	156.0	2.1
			158.6	86.4

Nuclear data used were taken from the National Nuclear Data Center's Online Archive [10].

Table 3
Summary of measured data for tellurium radioisotopes: ^{119g}Te, ^{119m}Te, ^{118}Te, ^{121m}Te, ^{121g}Te, and ^{123m}Te.

Energy (MeV)	ΔEnergy (MeV)	Te-119 g σ (mb)	Δσ (mb)	Te-119 m σ (mb)	Δσ (mb)	Te-118 σ (mb)	Δσ (mb)	Te-121 m σ (mb)	Δσ (mb)	Te-121 g σ (mb)	Δσ (mb)	Te-123 m σ (mb)	Δσ (mb)
67.2	0.2	34.4	3.7	60.7	6.6	97.4	11	20.2	2.2	10.5	1.1	2.5	0.3
59.6	0.4	57.4	6.5	109	12	102	12	26.7	3.0	13.9	1.6	3.3	0.4
51.2	0.6	79.0	9.6	135	17	157	20	37.2	4.5	18.3	2.2	4.2	0.5
43.6	0.9	57.5	7.7	98.2	13.1	262	36	63.5	8.5	27.2	3.6	5.1	0.7
35.6	1.3	179	26	288	42	61.4	10	216	32	83.0	12.1	7.0	1.0
33.6*	1.9	161	17	265	29	65.3	8	190	21	71.3	7.7	5.8	0.6
25.7*	0.7	172	20	203	23	–	–	239	27	130	15	7.7	0.9
20.7*	1.2	12.5	1.5	11.8	1.4	–	–	95.6	11.7	60.2	7.4	12.3	1.5
16.7*	2.1	–	–	–	–	–	–	30.0	4.0	19.7	2.6	17.8	2.4
12.0*	2.6	–	–	–	–	–	–	152	22	118	17	74.1	10.8

* Values below 34 MeV are associated with the second irradiation experiment.

Table 4
Summary of measured data for tin and antimony radioisotopes: ^{117m}Sn, ^{117}Sb, ^{118m}Sb, ^{120m}Sb, ^{122}Sb.

Energy (MeV)	ΔEnergy (MeV)	Sn-117 m σ (mb)	Δσ (mb)	Sb-117 σ (mb)	Δσ (mb)	Sb-118 m σ (mb)	Δσ (mb)	Sb-120 m σ (mb)	Δσ (mb)	Sb-122 σ (mb)	Δσ (mb)
67.2	0.2	7.7	0.8	187	20	46.8	5.3	40.0	4.7	49.1	5.7
59.6	0.4	7.4	0.8	266	30	42.6	5.0	46.9	5.7	56.7	6.9
51.2	0.6	8.8	1.1	172	21	45.5	5.8	53.1	6.9	63.9	8.3
43.6	0.9	7.1	1.0	5.7	0.8	25.3	3.5	45.7	6.4	70.3	9.8
35.6	1.3	3.7	0.5	0.14	0.03	21.5	3.4	32.2	4.9	77.2	11.7
33.6*	1.9	3.5	0.4	0.12	0.03	1.5	0.2	29.1	3.4	69.0	7.9
25.7*	0.7	4.4	0.5	0.07	0.03	–	–	23.1	2.8	59.6	7.2
20.7*	1.2	2.0	0.2	–	–	–	–	12.2	1.6	43.7	5.6
16.7*	2.1	0.5	0.1	–	–	–	–	3.6	0.5	19.8	2.8
12.0*	2.6	–	–	–	–	–	–	0.1	0.0	1.3	0.3

* Values below 34 MeV are associated with the second irradiation experiment.

3.2. ^{121m}Te and ^{121g}Te

The 212.2 keV line was used to determine the quantity of ^{121m}Te produced. Quantification of the cumulative or independent excitation functions for ^{121g}Te production is more difficult, as 88.6% of the ^{121m}Te decays to the ground state, decreasing the available signal. As a result, measured ^{121m}Te produced was analytically combined with the ^{121g}Te result to obtain the reported value for directly produced ^{121g}Te.

For both isomers of ^{121}Te, the data of Takacs et al. [7] are in very good agreement with our results. In the case of ^{121m}Te, the data of Batij et al. [20] and Elbinawi et al. [16] are also in good agreement with data presently reported. For ^{121g}Te, the situation is similar, and the newer data of Singh et al. [13] differ markedly in magnitude from those measured by other authors. The datasets of Lagunas-Solar et al. [11] and Yi and Miller [12] are in poor agreement with all other datasets reported for both reactions. All prior datasets are compared with our reported values in Figs. 4 and 5.

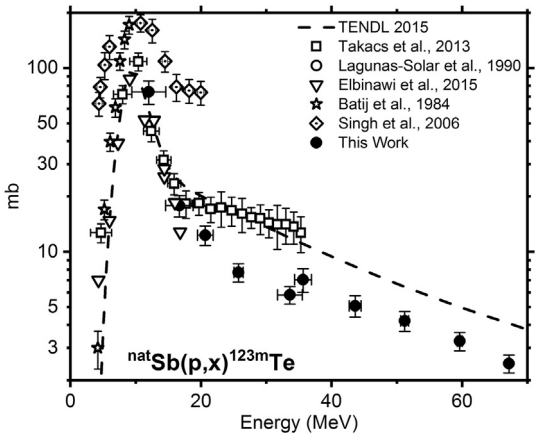

Fig. 1. Comparison of measured data from [7,11,16,20,13] and TENDL 2015 [19] with measured data for the ^{nat}Sb(p,x)^{123m}Te reaction.

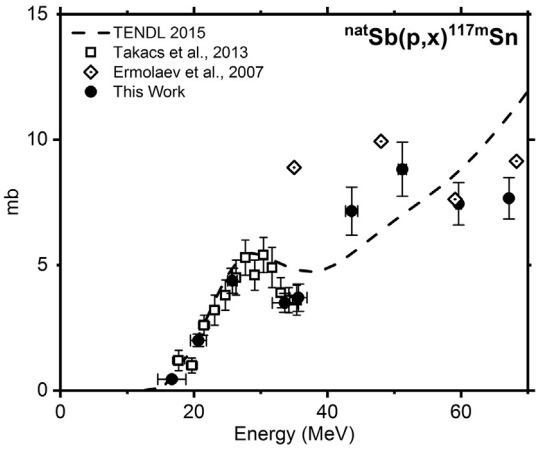

Fig. 2. Comparison of measured data from [11,17] and TENDL 2015 [19] with measured data for the ^{nat}Sb(p,x)^{117m}Sn reaction.

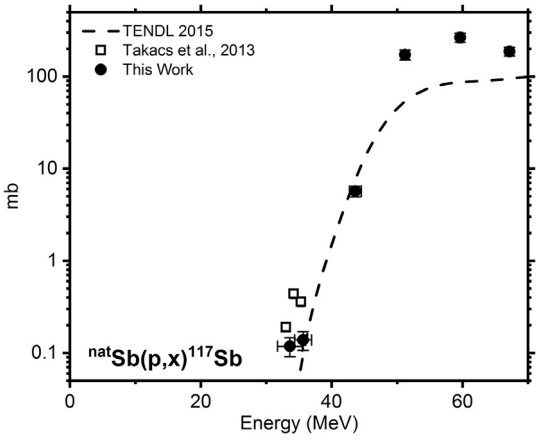

Fig. 3. Comparison of measured data from [7] and TENDL 2015 [19] with measured data for the ^{nat}Sb(p,x)^{117}Sb reaction.

3.3. ^{118}Te

The decay of ^{118}Te to ^{118g}Sb is 100% by electron capture with no accompanying gamma-rays, bypassing the isomer ^{118m}Sb ($t_{1/2}$ = 5.0 h). Both isomers of ^{118}Sb decay 100% to stable 118Sn. The decay of ^{118g}Sb does have an observable gamma-ray

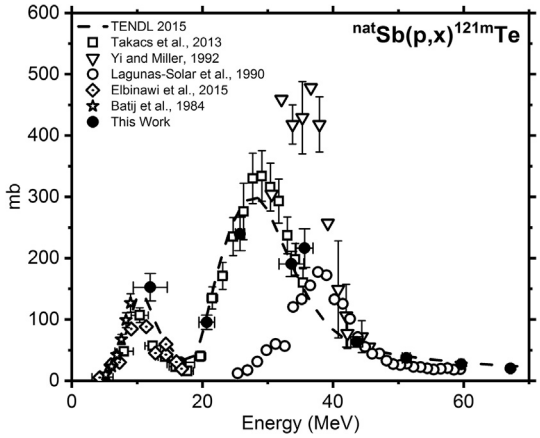

Fig. 4. Comparison of measured data from [7,11,16,20,12] and TENDL 2015 [19] with cumulative measured data for the ^{nat}Sb(p,x)^{121m}Te reaction.

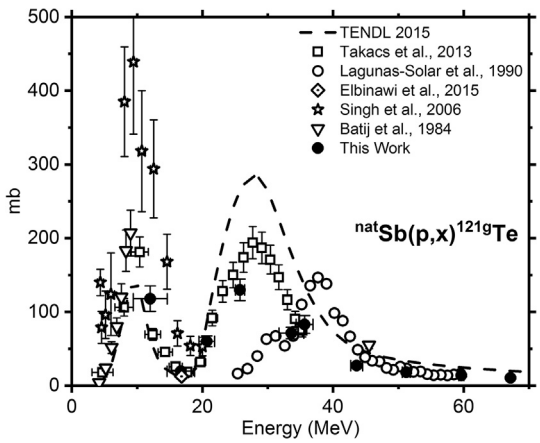

Fig. 5. Comparison of measured data from [7,11,16,20,13] and TENDL 2015 [19] with cumulative measured data for the ^{nat}Sb(p,x)^{121g}Te reaction.

(1229.3 keV, 2.5%), which was used to quantify the production of ^{118}Te. However, ^{118m}Sb was produced directly in the irradiation and emits at 1229.6 keV gamma-ray (100%), so it was necessary to remove its contribution. Only counts after the foils were shipped back to LANL were used to quantify ^{118}Te. This is two days after the end of irradiation for the 35 MeV run and three days later for the 68 MeV run, or a minimum of 10 half-lives of ^{118m}Sb from the end of irradiation. Once secular equilibrium is reached in the decay of ^{118}Te to ^{118g}Sb, the decay can be represented by the half life of ^{118}Te and the energy of the gamma transition from ^{118g}Sb. The fit to the decay curve is consistent with no other components present in the sample, resulting in a photopeak free from signal contamination. Only the data of Takacs et al. [7] are in good agreement with the values reported here and shown in Fig. 6.

3.4. ^{119m}Te and ^{119g}Te

Both the 271 keV and 1213 keV peaks were used to quantify ^{119m}Te, and ^{119g}Te was quantified using its 644 and 700 keV peaks. Each photopeak produced pairs of values in good agreement with one another, and logarithmic fits of decay curves showed no evidence of photopeak contamination. These two radionuclides are a potential source of generators of ^{119}Sb, so the measured magnitude of the excitation functions at a few hundred millibarns is encouraging from a yield perspective. As has been the case elsewhere, only the data of Takacs et al. [7] are in satisfactory

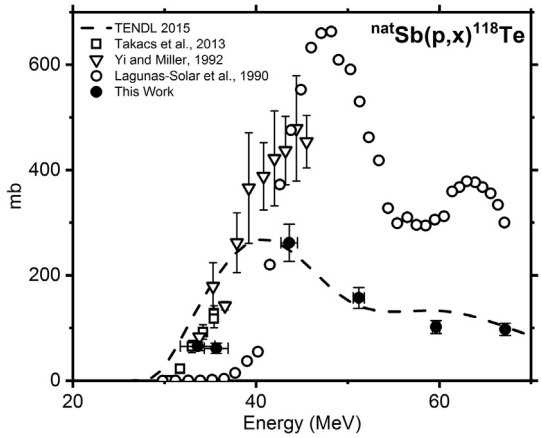

Fig. 6. Comparison of measured data from [7,11,12] and TENDL 2015 [19] with measured data for the ^{nat}Sb(p,x)^{118}Te reaction.

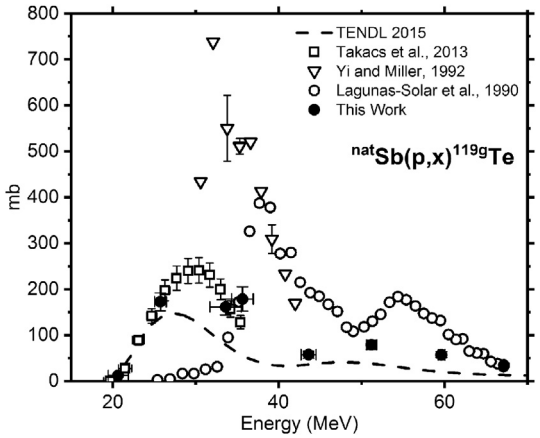

Fig. 8. Comparison of measured data from [7,11,12] and TENDL 2015 [19] with measured data for the ^{nat}Sb(p,x)^{119g}Te reaction.

agreement with values reported here. Newly measured data represent for the first time the shape of the ^{123}Sb(p,5n) component of the excitation function. This target isotope's natural abundance (43%) is slightly lower than that of ^{121}Sb (57%), but it still offers the potential for an attractive production route to ^{119}Sb at between 40 and 70 MeV. The data measured in this work are summarized in Figs. 7 and 8.

3.5. ^{120m}Sb

Quantification of ^{120m}Sb is facilitated by three different prominent gamma lines at 197, 1023, and 1171 keV. The Takacs et al. data [7] are in excellent agreement with our measured values as shown in Fig. 9, and both datasets show a more pronounced decline transition region between the ^{121}Sb(p,pn)^{120m}Sb and ^{123}Sb(p,p3n)^{120m}Sb excitation functions than is predicted by TALYS [19]. The decay of ^{120m}Sb by electron capture completely (100%) bypasses ^{120g}Sb ($t_{1/2}$ = 15.89 min), which could not be quantified due to the delay between the end of irradiations and the start of counting and the relatively small intensity (1.69%) of its sole characteristic photopeak at 1171 keV). However, ^{120m}Sb poses no threat to the radioisotopic purity of generator-based produced ^{119}Sb because ^{120}Te (0.09%) is stable.

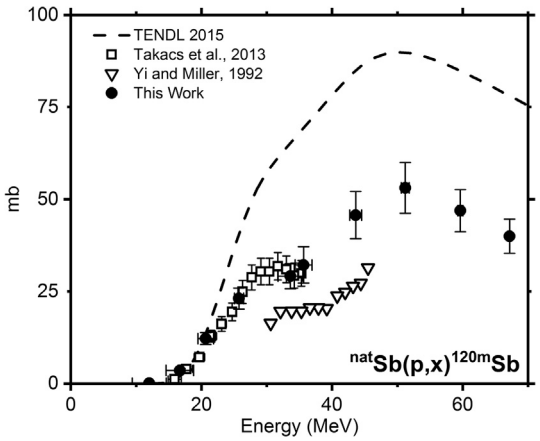

Fig. 9. Comparison of measured data from [7,11,12] and TENDL 2015 [19] with measured data for the ^{nat}Sb(p,x)^{120m}Sb reaction.

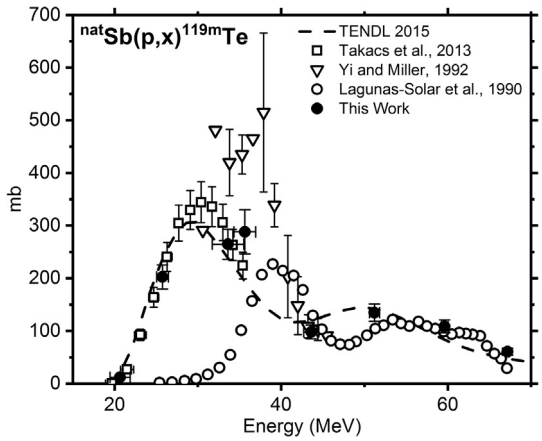

Fig. 7. Comparison of measured data from [7,11,12] and TENDL 2015 [19] with measured data for the ^{nat}Sb(p,x)^{119m}Te reaction.

3.6. ^{122}Sb

The 564 keV photopeak from the β^- branch (98%) of ^{122}Sb's ground state was used to quantify its excitation function. The previously published results of the Takacs group [7] and the shape of the function predicted by the TALYS code [19] are both in excellent agreement with presently reported values. The data of Yi and Miller [12] are inexplicably shifted in magnitude and in poor agreement with the remaining measured data plotted in Fig. 10.

3.7. ^{118m}Sb

Both isomers of ^{118}Sb (^{118g}Sb $t_{1/2}$ = 3.6 min) decay entirely by electron capture, with the ground state emitting a strong positron branch ($E_{<\beta+>}$ = 1188 keV, 73.2%). This fact has been employed to suggest in vivo generators of ^{118}Te/^{118g}Sb [21], which are however not useful for the production of therapeutic radionuclides of tin or antimony. Instead, unavoidable contamination of ^{118}Te produced by the ^{121}Sb(p,4n) and ^{121}Sb(p,6n) reactions will necessitate a brief delay in injection of compounds radiolabeled by generator-produced ^{119}Sb to allow co-eluted ^{118g}Sb to decay.

The useful cross section for production of ^{118m}Sb occurs almost entirely above 30 MeV, well above the energy range of prior measurements made for proton irradiations of antimony targets. Data reported here suggest a strongly increasing function between 30

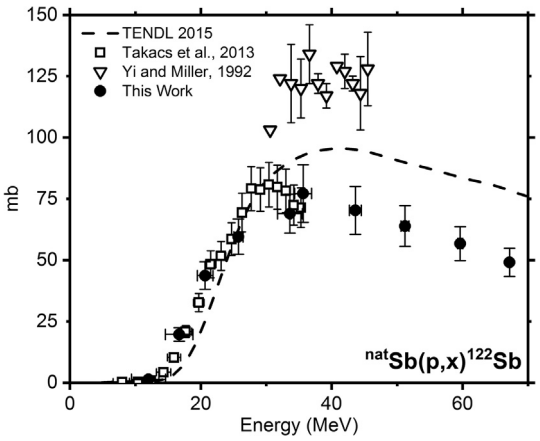

Fig. 10. Comparison of measured data from [7,21] and TENDL 2015 [19] with measured data for the $^{nat}Sb(p,x)^{122}Sb$ reaction.

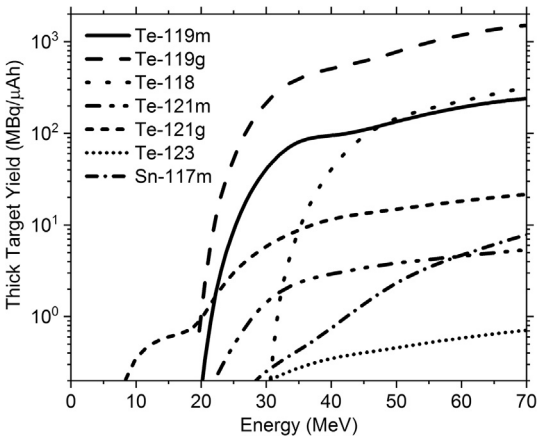

Fig. 12. Instantaneous thick target yields for proton-induced reactions producing radioisotopes of tellurium and tin, calculated using data in the current work and that of Takacs et al. [7]. Radioisotopes of antimony are not plotted for clarity and because of their irrelevance to the production of ^{119}Sb and ^{117m}Sn, the primary motivations for this work.

and 40 MeV, as do data from Takacs et al. [7] and the predictions of the TALYS code [19]. The data are summarized in Fig. 11 below.

3.8. Thick target, instantaneous yields

Yields from infinitesimally short irradiations were calculated using data measured in this work and additionally the datasets from Takacs et al. [7], which is generally in agreement with the results reported here. This yield figure is understood not to incorporate the effect of radioactive decay on produced radionuclides during the period of irradiation; in other words, the length of bombardment is assumed to be short relative to the half-life of the radionuclides in question. The results of these calculations for tellurium and tin are presented below in Fig. 12.

Optimal radioisotopic purity of $^{119(m+g)}Te$ is achieved with entrance energies of 30 MeV or less. However, the additional yield afforded by the $^{123}Sb(p,5n)^{119(m+g)}Te$ reactions may motivate the use higher incident energies given that tellurium should be chemically separable from antimony and that no radioisotopes of tellurium will decay to radioisotopes of antimony in a manner problematic for a $^{119}Te/^{119}Sb$ generator.

This work's expansion of the energy range of data available considering production of ^{117m}Sn reveals an increase in achievable yield up to and presumably well beyond 70 MeV. The current work does not reveal to what extent production of ^{117m}Sn might be limited by coproduction of radioisotopic impurities. Though ^{121}Sn is likely formed, as the Q value of the $^{123}Sb(p,2pn)$ reaction is only 15 MeV, the HPGe spectrometry used to quantify residuals in this work would not have detected ^{121m}Sn ($t_{1/2}$ = 43.9 y, 77.6% IT, 22.4% ß$^-$) or ^{121g}Sn ($t_{1/2}$ = 27.03 h, 100% ß$^-$), as neither isomer emits a γ-ray with an energy higher than 37.15 keV. The potentially problematic $^{121}Sb(p,8n)^{113m}Sn$ reaction will manifest itself above approximately 65 MeV, but ^{113m}Sn ($t_{1/2}$ = 115.09 d, 100% EC) was not observed in the counting performed on our irradiated samples.

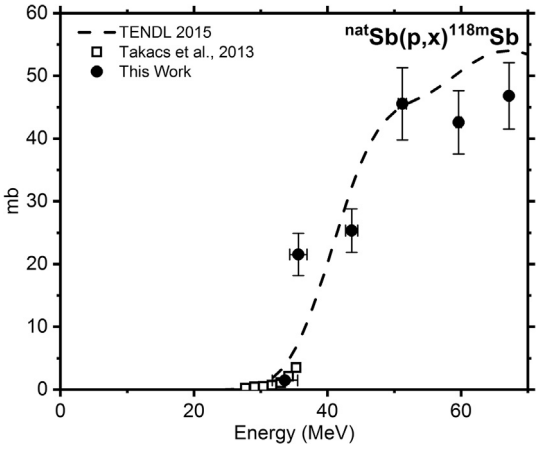

Fig. 11. Comparison of measured data from [7] and TENDL 2015 [19] with measured data for the $^{nat}Sb(p,x)^{118m}Sb$ reaction.

4. Conclusions

Measurements reported above are the first extension of proton-induced data above 50 MeV for reactions on antimony targets. They are relevant to current efforts to produce ^{119}Sb as a potential therapeutic radionuclide in a convenient generator using ^{119}Te as the parent, and to the ongoing international effort to make therapeutic quantities of ^{117m}Sn available for trials with radiotherapeutic compounds. Previously measured data for these reactions is often discrepant, and measurements like those reported here offer confidence that yield and purity predictions can me made accurately prior to placing a target in beam.

Acknowledgements

This study was carried out under the auspices of the National Nuclear Security Administration of the U.S. Department of Energy at Los Alamos National Laboratory under Contract No. DE-AC52-06NA253996 with partial funding by the US DOE Office of Science via an award from The Isotope Development and Production for Research and Applications subprogram in the Office of Nuclear Physics. We gratefully acknowledge the skilled technical assistance of LANL C-NR staff and are indebted to Randy Kemmler and Spencer Davis for their invaluable technical services.

References

[1] H. Uusijärvi, P. Bernhardt, F. Rösch, H.R. Maecke, E. Forssell-Aronsson, Electron- and positron-emitting radiolanthanides for therapy: aspects of dosimetry and production, J. Nucl. Med. 47 (2006) 807–814.
[2] G. Makrigiorgos, S.J. Adelstein, A.I. Kassis, Auger electron emitters: insights gained from in vitro experiments, Radiat. Environ. Biophys. 29 (1990) 75–91, http://dx.doi.org/10.1007/BF01210552.
[3] Peter Bernhardt, Eva Forssell-Arons, P. Bernhardt, E. Forssell-Aronsson, L. Jacobsson, G. Skarnemark, Peter Bernhardt, Eva Forssell-Arons, P. Bernhardt, E.

Forssell-Aronsson, L. Jacobsson, G. Skarnemark, Low-energy electron emitters for targeted radiotherapy of small tumours, Acta Oncol. 40 (2001) 602–608, http://dx.doi.org/10.1080/028418601750444141.
[4] H. Thisgaard, M. Jensen, Production of the Auger emitter ^{119}Sb for targeted radionuclide therapy using a small PET-cyclotron, Appl. Radiat. Isot. 67 (2009) 34–38.
[5] Z.H. Oster, P. Som, S.C. Srivastava, R.G. Fairchild, G.E. Meinken, D.Y. Tillman, D. F. Sacker, P. Richards, H.L. Atkins, A.B. Brill, The development and in-vivo behavior of tin containing radiopharmaceuticals-II. Autoradiographic and scintigraphuc studies in normal animals and in animal models of bone disease, Int. J Nucl. Med. Biol. 12 (1985) 175–184.
[6] B. Ponsard, S.C. Srivastava, L.F. Mausner, F.F. (Russ) Knapp F.F., M.A. Garland, S. Mirzadeh, Production of Sn-117m in the BR2 high-flux reactor, Appl. Radiat. Isot. 67 (2009) 1158–1161, http://dx.doi.org/10.1016/j.apradiso.2009.02.023.
[7] S. Takacs, M.P. Takacs, a. Hermanne, F. Tarkanyi, R. Adam Rebeles, S. Takács, M. P. Takács, a. Hermanne, F. Tárkányi, R. Adam Rebeles, S. Takacs, M.P. Takacs, a. Hermanne, F. Tarkanyi, R. Adam Rebeles, Cross sections of proton induced reactions on ^{nat}Sb, Nucl. Instrum. Meth. Phys. Res. Sect. B Beam Interact. Mater. Atoms 297 (2013) 44–57, http://dx.doi.org/10.1016/j.nimb.2012.12.010.
[8] J.F. Ziegler, J.P. Biersack, M.D. Ziegler, SRIM – the stopping and range of ions in matter, Nucl. Instrum. Methods Phys. Res. B. 268 (2010) 1818–1823. http://www.srim.org.
[9] R. Capote-Noy, F.M. Nortier, Improvements in charged-particle monitor reactions and nuclear data for medical isotope production, in: INDC(NDS)-0591, IAEA International Nuclear Data Committee, Vienna, Austria, 2011.
[10] NUDAT2, http://www.nndc.bnl.gov/nudat2/. (Accessed July 2017).
[11] M.C. Lagunas-Solar, O.F. Carvacho, S.-T. Yang, Y. Yano, Cyclotron production of PET radionuclides: ^{118}Sb (3.5 min; β+ 75%; EC 25%) from high-energy protons on natural Sb targets, Appl. Radiat. Isot. 41 (1990) 521–529, http://dx.doi.org/10.1016/0883-2889(90)90033-D.
[12] J.H. Yi, D.a. Miller, Cross sections of ^{nat}Sb(p,x) reactions for 30-46 MeV protons, Appl. Radiat. Isot. 43 (1992) 1103–1106.
[13] B.P. Singh, M.K. Sharma, M.M. Musthafa, H.D. Bhardwaj, R. Prasad, A study of pre-equilibrium emission in some proton- and alpha-induced reactions, Nucl. Instrum. Meth. Phys. Res. Sect. A Accel. Spectrom. Detect. Assoc. Equip. 562 (2006) 717–720, http://dx.doi.org/10.1016/j.nima.2006.02.030.
[14] V.G. Batij, E.A. Skakun, Cross Sections of (p,n) reaction on 117-, 118-, 122-, 124-Sn, in: Conf. Nucl. Data Sci. Technol., Nice, France, 2007: p. 1325.
[15] S.V. Ermolaev, B.L. Zhuikov, V.M. Kohanyuk, S.C. Srivastava, Production yields of 117mSn from natural antimony target in proton energy range 145–35 MeV, J. Labeled Compd. Radiopharm. 50 (2007) 611–612.
[16] A. Elbinawi, M. Al-abyad, K.E. Abd-Elmageed, K.F. Hassan, F. Ditroi, Proton induced nuclear reactions on natural antimony up to 17 MeV, Radiochim. Acta. (2015) 1–6, http://dx.doi.org/10.1515/ract-2015-2483.
[17] J.W. Engle, S.G. Mashnik, J.W. Weidner, L.E. Wolfsberg, M.E. Fassbender, K. Jackman, A. Couture, L.J. Bitteker, J.L. Ullmann, M.S. Gulley, C. Pillai, K.D. John, E.R. Birnbaum, F.M. Nortier, Cross sections from proton irradiation of thorium at 800 MeV, Phys. Rev. C. 88 (2013) 14604.
[18] Y.E. Titarenko, V.F. Batyaev, M.A. Butko, D.V. Dikarev, S.N. Florya, K.V. Pavlov, A. Y. Titarenko, R.S. Tikhonov, V.M. Zhivun, A.V. Ignatyuk, S.G. Mashnik, A. Boudard, S. Leray, J.-C. David, J. Cugnon, D. Mancusi, Y. Yariv, H. Kumawat, K. Nishihara, N. Matsuda, G. Mank, W. Gudowski, Verification of high-energy transport codes on the basis of activation data, Phys. Rev. C. 84 (2011) 1–19.
[19] D.M. Koning A J, Hilaire S, TALYS 1.8. http://www.talys.eu. (Accessed March 2016).
[20] V.G. Batij, E.A. Skakun, O.A. Rastrepin, Y.N. Rakivnnenko, Excitation functions of Sb-121(p, n)Te-121m, g and Sb-123(p, n)Te-123m reactions, Izv. Ross. Akad. Nauk. Seriya Fiz. 48 (1984) 197.
[21] D.A. Miller, S. Sun, J.H. Yi, Preparation of a ^{118}Te/^{118}Sb Radionuclide Generator, J. Radioanal. Nucl. Chem. 160 (1992) 467–476.